Adsorption of Membrane-Associated Proteins to Lipid Bilayers Studied with an Atomic Force Microscope: Myelin Basic Protein and Cytochrome *c*

Henning Mueller,[†] Hans-Jürgen Butt,*[,‡] and Ernst Bamberg[†]

Max-Planck-Institut für Biophysik, Kennedyallee 70, D-60596 Frankfurt(Main), Germany, and Institut für physikalische Chemie, Universität Mainz, Welderweg 11, D-55099 Mainz, Germany

Received: November 17, 1999

Atomic force microscopy was used to study the structure of two membrane-associated proteins adsorbed to various supported phospholipid bilayers in physiological buffer. The aim was (a) to develop a preparation for the investigation of membrane-associated proteins at high resolution under native conditions and (b) to obtain information about the factors that determine the adsorption process and the structure of adsorbed proteins. Therefore, solid-supported membranes were formed on mica by spontaneous vesicle adsorption and spreading. Once a homogeneous, pinhole-free bilayer was formed, solutions containing the proteins at appropriate concentrations were applied. The two positively charged proteins chosen were myelin basic protein (MBP), which plays an essential role in the formation of functional myelin, and cytochrome *c*. On charged bilayers, MBP applied at concentrations of 0.5−50 μg/mL formed aggregates of defined height (1.9 ± 0.2 nm on negatively and 2.7 ± 0.2 nm on positively charged lipids), which at high concentration covered the entire bilayer. These aggregates are probably monomolecular layers of MBP. On neutral lipid adsorbed MBP formed irregular aggregates. Cytochrome *c* showed a different adsorption: On negatively charged lipid it formed aggregates of defined, monomolecular height (3.3 ± 0.2 nm). On neutral bilayers small aggregates were observed. On positively charged lipid no adsorption was observed at all. These results indicate that (a) the adsorption of cytomchrome *c* can be interpreted in terms of a dominating electrostatic interaction; (b) MBP adsorption to lipid bilayers is not exclusively electrostatically driven and depends on the specific lipid bilayer composition; (c) the structure of adsorbed aggregates indicates a strong protein−protein interaction.

Introduction

Membrane-associated proteins play an essential role in many processes in cells, such as respiration and regulation. Despite their importance in many cases, detailed information about the adsorption process and about the structure of proteins once they are associated with membranes is lacking. Adsorption is usually studied with optical techniques (e.g., ellipsometry, surface plasmon spectroscopy[1], X-ray or neutron reflectometry[2], or the quartz microbalance[3]). With these techniques the thickness of adsorbed layers can be measured with subnanometer resolution. The lateral resolution is, however, in the millimeter range. High-resolution structural studies by electron microscopy are difficult because lipid bilayers are only stable in aqueous environment. Therefore it is desirable to have complementary techniques.

One such technique is atomic force microscopy (AFM). Atomic force microscopes can be operated in liquid environment. Their potential resolution is better than 1 Å in the vertical and roughly a few nanometers (for single objects) in the lateral direction. A requirement for good resolution is a flat and smooth substrate. For this paper we developed a preparation suitable for AFM to study membrane-associated proteins on lipid bilayers. Continuous, pinhole-free acidic, zwitterionic, and basic lipid bilayers were formed on mica. Then the adsorption of two membrane-associated proteins, myelin basic protein (MBP) and cytochrome *c*, was studied.

MBP is essential for the formation of the myelin sheath. The myelin sheath of the nervous system consists of flat sheets extending from oligodendrocyte cells that enwrap selected axons multiple times. In this way they form compact multilamellar lipid layers and provide for electrical insulation of the axon which is necessary for saltatory signal transduction.[4]

The ability to express MBP is indispensable for myelin compaction.[5] Numerous MBP isomers and isoforms are created by different exon splicing and various posttranslational modifications[6] with probably different roles in the myelin compaction process.[7] It is generally accepted that at least two MBP isoforms act as intermembrane adhesion proteins; they help to form and stabilize the major dense lines by cross-linking the cytoplasmic membrane leaflets.[8−10]

The interaction mechanism between MBP and the myelin membrane is important to understand the myelination process. Because specific interaction between the transmembrane proteolipid proteins and (the cytoplasmic) MBP could not be established,[11] and it is unlikely that MBP is anchored to the membrane via phosphatidylinositol bisphosphate,[12] attention has turned to investigating direct interactions between MBP and the lipid bilayer membrane.

MBP-induced vesicle aggregation has been intensively studied,[9,13,14] providing evidence for MBP ability of lipid bilayer (noncovalent) cross-linking. Although the importance of electrostatic contributions in MBP−lipid bilayer interaction seems well established, presence and magnitude of a hydrophobic component are still debated.[10,15−18]

Of equal importance is information on MBP structure and its localization on or within the bilayer. Efforts to crystallize

* To whom correspondence should be addressed. Phone: +49-6131-392-3930; fax: +49-6131-39-2940; email: butt@wintermute.chemie.uni-mainz.de.
[†] Max-Planck Institut für Biophysik.
[‡] Institut für physikalische Chemie.

10.1021/jp9940856 CCC: $19.00
Published on Web 04/15/2000

MBP have so far not been successful.[19] X-ray diffraction and neutron scattering data were collected on MBP−lipid multilayers transferred by the Langmuir−Blodgett technique[20] to solid substrates. Results indicate that MBP does not penetrate beyond the headgroup region and extends approximately 1.5 nm above the membrane surface.[16,21] Small-angle X-ray diffraction and nuclear magnetic resonance studies have shown MBP to exhibit a flexible coil structure in aqueous solution.[22] Differential scanning calorimetry used to study the phase behavior of lipid bilayers interacting with MBP showed MBP adsorption to decrease the phase transition temperature and enthalpy in various lipid bilayer systems.[23,24] This was interpreted as some MBP intercalation into the lipid bilayer. Whether negatively charged and zwitterionic lipids demix on MBP binding is still discussed.[18,25,26]

From an electron microscopy study of randomly oriented bovine 18.5-kDa MBP (C1 isoform) molecules adsorbed to a lipid monolayer at the air−water interface, Beniac et al.[27] report a "C" shape for the MBP molecule of outer radius 5.5 nm and 4.7 nm height.

We have investigated the adsorption of MBP to planar lipid bilayers of various compositions formed on mica by vesicle fusion. Therefore, we used the most basic isoform (C1) of bovine MBP of 18.5 kDa molecular mass, which elutes in the last peak on an anion-exchange column. As simple models for the myelin membrane, lipid bilayers consisting of zwitterionic egg phosphatidylcholine (EPC) and 10−20% (weight) of acidic dioleoylphosphatidylserine (DOPS) have been used before.[18,28] We chose a lipid composition containing 14% (weight) DOPS, 56% EPC, and 30% cholesterol. The high cholesterol content is typically found in myelin membranes.[29] For comparison, adsorption to purely zwitterionic bilayers (70% zwitterionic lipids, 30% cholesterol) and to bilayers containing 14% basic instead of acidic lipids was also studied. Direct information on how MBP adsorbs to such planar lipid bilayers was obtained. Furthermore, the mechanical properties of the bilayer with and without adsorbed MBP were studied by force-versus-distance measurements with the AFM cantilever. Thus it was possible to investigate the effect of MBP adsorption on the mechanical properties of the lipid bilayer.

Cytochrome *c* is a basic peripheral membrane protein that shuttles electrons between cytochrome bc_1 and cytochrome *c* oxidase in the mitochondrial respiratory chain. Its structure has been determined by X-ray diffraction.[30] Just like MBP, much work has been dedicated to elucidate the interaction of cytochrome *c* with lipid bilayers. At least the initial step in cytochrome *c* adsorption is of electrostatic nature.[31] Results from more recent experiments have been interpreted in such a way that after adsorption, cytochrome *c* changes its conformation and can partly or completely penetrate into the hydrophobic core of the bilayer,[32,33] although some spectroscopic and X-ray diffraction studies argue against such a penetration.[16,34] In this work, cytochrome *c* adsorption served as a useful comparison with MBP adsorption because cytochrome *c* is also a basic peripheral membrane protein with a function different from MBP, and a known structure.

For comparison, we also studied the adsorption of bovine serum albumin (BSA) to those lipid bilayers. BSA is a typical water-soluble protein of 66.5 kDa molecular mass and constitutes approximately half of the total mammalian blood serum protein. It serves as a complex former with fatty acids to facilitate their transport in the circulatory system.[35]

Materials and Methods

Reagents. All chemicals were of analytical grade and were used without further treatment except chloroform used for solvation of lipids, which were IR grade (Merck, Darmstadt, Germany). Potassium chloride, potassium hydroxide, and potassium dihydrogen phosphate were also purchased from Merck. Sodium chloride was purchased from Fluka, Neu-Ulm, Germany. EPC, DOPS, and cholesterol were purchased from Avanti Polar Lipids, Alabaster, AL. BSA (order no. A-2153), horse heart cytochrome *c* (C-7752), and dioleoyl triammonium salts (DOTAP) were purchased from Sigma, Steinheim, Germany. Cholesterol, EPC, and DOPS were dissolved in IR-grade chloroform and stored at −20 °C. DOTAP was dissolved in IR-grade chloroform and stored at −80 °C. Buffer 1 (150 mM NaCl, 5 mM KH_2PO_4, pH 7.4 titrated with KOH) was used as a standard buffer for AFM measurements. Buffer 2 [5 M NaCl, pH ∼6 (uncontrolled)] was used as a high ionic strength buffer. MBP was purified from bovine brain as described before[27,36] and kept at −80 °C until use.

Atomic Force Microscopy. Measurements were carried out with a commercial AFM (NanoScope 3, Digital Instruments, Santa Barbara, CA) and Si_3N_4 cantilevers (Digital Instruments, length 200 μm, width 40 μm, estimated thickness 0.6 μm, radius of tip curvature ∼20−60 nm[37]). Cantilever spring constants were individually determined by moving them against a reference cantilever. The reference cantilever was calibrated by a method described by Cleveland et al. and Preuss and Butt.[38] Spring constants were in the range of 0.06−0.14 N/m. Horizontal scanner calibration was performed by imaging 10 μm grids supplied by the manufacturer. In the vertical direction the scanner was calibrated as described by Jaschke and Butt.[39] Images were taken in contact mode in buffer, using a standard fluid cell. The setup allows the recording of deflection images and height images. For height images, displacement of the *z* piezo through a feedback loop using tip deflection as an input is recorded. These data supply information on sample height. For deflection images, the deflection of the tip is recorded at low feedback. No height information can be deduced from these data. We use deflection images when we want to emphasize sample shape, because contrast in deflection images is usually better than in the corresponding height images. Recording one image took approximately 2 min.

Force-versus-Distance Measurements. A detailed explanation of force-versus-distance measurements carried out at individual points on the surface can be found in Mueller et al.[36] Briefly, the tip with cantilever is positioned above a defined point on the surface. Then the surface is moved periodically toward and away from the tip by applying voltage ramps to the *z* piezo displacement. If surface forces are present, they will cause a cantilever deflection before the tip is in contact with the surface. To obtain a force-versus-distance curve (from now on called a force curve), cantilever deflection as a function of piezo displacement is recorded. From this, a force curve is calculated by multiplying cantilever deflection with the spring constant of the cantilever to obtain the force, and adding *z* piezo displacement and cantilever deflection to obtain the distance from contact. Recording a force curve took 1 s. Analysis of force curves yields information on local surface forces,[40] which is valuable for interpretation of surface processes.

Often, an offset of 0.5−1 nm between the point of contact for approaching and retracting force curves was observed. This is probably caused by a friction effect.[41] In these cases we have separately calibrated the z origins for approach and retraction.

TABLE 1: Composition of Three Types of Bilayers Investigated[a]

	acidic (I)	zwitterionic (II)	basic (III)
cholesterol	30	30	30
EPC	56	70	56
DOPS	14	−	−
DOTAP	−	−	14

[a] Numbers in the table indicate the weight percentage of the phospholipid that was used for bilayer types I, II, and III.

Sample Preparation. Lipid vesicles for vesicle fusion on mica were prepared as follows: the dissolved lipids were mixed in the desired proportions (Table 1) and the solvent evaporated under N_2. Buffer 1 was added to the obtained lipid film to produce a 5 mg/mL suspension that was thoroughly sonicated (G112SP1T sonicator, Laboratory Supplies Co., Hicksville, NY) until the suspension became opalescent. Bilayers formed from vesicles that spontaneously spread on solid substrates have been described before.[42,43] We used the following protocol: the AFM head equipped with a standard fluid cell (Digital Instruments) was mounted on freshly cleaved mica (Plano, Wetzlar, Germany) and the fluid cell was flushed with buffer 1. After 15−60 min, a 20 μm image of the mica surface was taken to ensure that it was clean. Then 100 μL of vesicle suspension briefly heated to 50 °C was injected. After 30−60 min, remaining vesicles in the bulk phase were rinsed away with 400 μL of buffer 1. After 10 min, another image and force curves at various points on the surface were taken to ascertain homogeneous coverage of the mica with the lipid bilayer (see *Results*). Afterward, 100 μL of MBP solution (0.5−50 μg/mL, ∼30 nM−3 μM) were injected. AFM images at various adsorption times were taken at room temperature (∼30 °C in the fluid cell after thorough equilibration). During scanning, the imaging force was adjusted to the smallest possible value while the image remained stable and clear. Such minimal imaging forces were typically 0.2 nN. In some instances the buffer was changed during the experiment. In these cases, at least 5 min passed before a new image could be taken because of drift of the deflection offset.

Results and Discussion

Lipid Bilayer Formation. Before vesicle injection, images of the mica surface were flat and showed no adsorbed material (Figure 1a). After vesicle adsorption times greater than 30 min, a flat surface was observed, with usually few specks on top (Figure 1b). The specks could not be rinsed away. The actual presence of the bilayer after vesicle adsorption was verified by taking force curves at different points on the surfaces. On mica, only a very short range repulsion (decay length approximately 0.2 nm, Figure 1c, inset) was observed before, and a small adhesion after contact (Figure 1c). After vesicles had been present, the tip experienced short-range repulsion (Table 2, Figure 1d), but at forces between 4 and 12 nN, the tip suddenly jumped onto the sample (Figure 1d). Jump-in distances and decay lengths of the repulsions on the studied surfaces are shown in Table 2. On retraction, adhesion was often (but not always) present.

Short-range repulsive forces have been observed between flat hydrophilic surfaces and between lipid bilayers before,[44−47] and they were termed hydration forces.[48] The origin of these forces is, however, controversial. On mica, the repulsion is probably due to the tip penetrating the thin layer of water and ions on the mica surface.[45] On the bilayer, an additional repulsive force could be caused by the fluctuating, protruding lipid molecules.[46,49] The fact that we observe different decay lengths on mica and on lipid bilayers indicates that indeed for lipid bilayers an additional effect has to be considered.

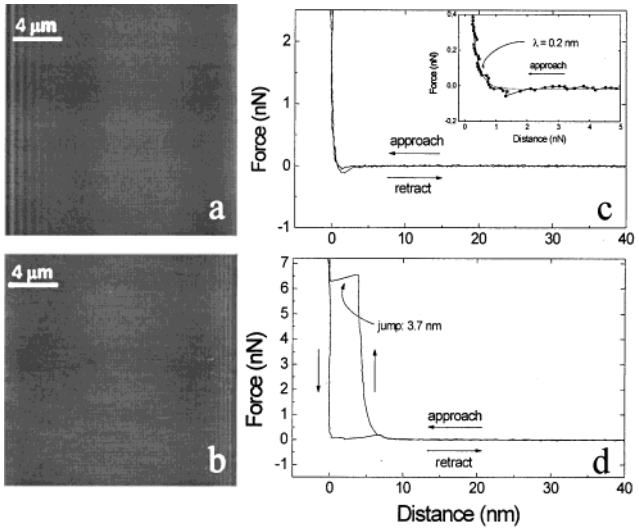

Figure 1. (a) Height image of freshly cleaved mica in buffer 1 and (b) after deposition of a lipid bilayer (type I). Both surfaces are flat, *z* scale is 5 nm black to white. (c) Typical force curve on bare mica. The *inset* zooms in onto the repulsion observed during approach. An exponential fit of the data (decay length: 0.2 nm) is also depicted. (d) Typical force curve after deposition of a type I lipid bilayer. The approaching tip first experiences exponential repulsion (decay length: 1.2 nm, not depicted), followed by a jump across 3.7 nm.

TABLE 2: Jump Distances (Corresponding to Bilayer Thickness) and Decay Lengths of Repulsion Observed during Approach on Each Bilayer and on Bare Mica

lipid mix	jump (nm)	decay length (nm)
I (acidic)	3.5 ± 0.2	1.20 ± 0.08
II (neutral)	3.9 ± 0.2	0.62 ± 0.04
III (basic)	4.4 ± 0.2	1.08 ± 0.09
bare mica		0.32 ± 0.03

We believe the jump-in is a penetration of the lipid bilayer by the tip (observed by Ducker and Clarke[50] on zwitterionic surfactants). From X-ray scattering experiments, the thickness of a fully hydrated pure EPC bilayer was determined to be 6.3 nm and a headgroup−headgroup distance of 4 nm has been reported.[47] This is consistent with the punch-through distances we have observed (Table 2). Because images of bilayers were flat, and identical characteristic force curves (Figure 1d) were found at any random position of the sample, we conclude that the mica was homogeneously covered by a lipid bilayer.

Mou et al.[43] were able to induce defects into dipalmitoylphosphatidylcholine (DPPC) bilayers by fast (200 Hz) scanning at high (30 nN) forces. We could not induce such defects into our EPC/cholesterol bilayers. The DPPC bilayers of Mou et al. were in the condensed phase (transition temperature T_m = 41 °C), whereas for EPC, T_m is approximately 5 °C.[51] Thus our mixed lipid bilayers were in the fluid phase and no stable defects could be formed.

For the bilayers containing fractions of lipids with positively or negatively charged headgroups (type I and type III bilayers), the question arises whether the negatively charged mica substrate causes an asymmetry in the distribution of charged lipid headgroups. In type I bilayers, one would expect to find more negative DOPS headgroups oriented toward the solution rather than the mica, whereas for type III bilayers, more positive DOTAP headgroups are expected to face the mica rather than the solution. Indeed, such an asymmetric distribution of charged

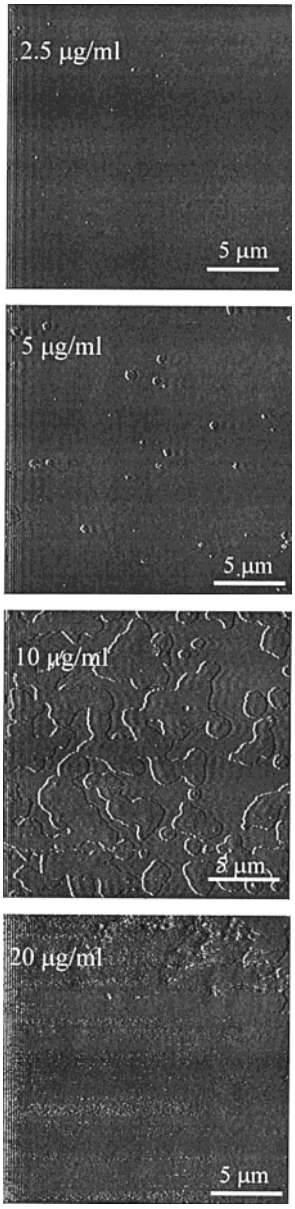

Figure 2. Deflection images of elevations observed on an acidic (type I) lipid bilayer 5 min after injection of MBP solution at different concentrations. The undulations to the right of the aggregates in the second and third image are scanning artifacts probably caused by contamination of the tip with protein, which is then amplified through the feedback loop. The artifacts did not disappear when scanning at slower speed. In the bottom image, contrast disappears during the scan, probably due to contamination of the tip with MBP. At concentrations greater than 20 μg/mL, contrast could usually not be obtained any more.

headgroups could be inferred from a series of experiments using a number of different methods by Käsbauer et al.[52] Their results showed that in low ionic strength buffer (20 mM HEPES, 20 mM NaCl, 0.5 mM EDTA, pH 7.0), the amount of anionic lipid in the bilayer leaflet facing the mica had decreased by 30% over 12 h. In buffer containing 500 mM NaCl, no asymmetries were found. Because our experiments usually lasted up to 5 h maximum and were carried out in 150 mM NaCl buffer, the effects of such an asymmetry in our system are probably small.

MBP Adsorption. The adsorption of MBP to lipid bilayers was studied in two ways: First, the adsorption time after which images were taken was kept constant and MBP solution of different concentrations was injected. Second, MBP adsorption was followed in time, keeping the concentration constant.

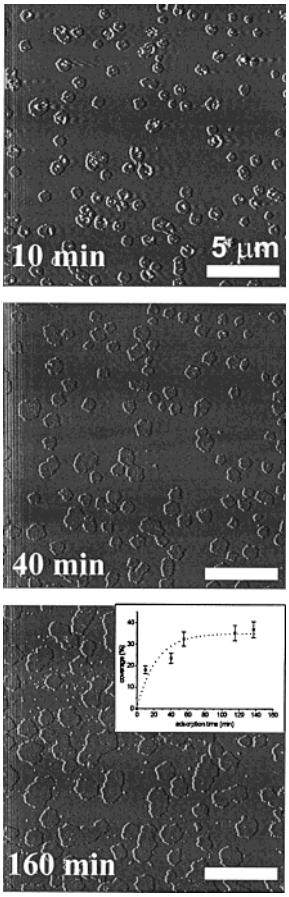

Figure 3. Deflection images of elevations observed on an acidic (type I) lipid bilayer at various times after injection of MBP solution (concentration: 5 μg/mL). Elevations can be observed to grow laterally and eventually fuse with their neighbors. The *inset* in the bottom image shows the relative coverage as a function of adsorption time. A function of type $A(1 - e^{-x/\lambda})$ was fitted to the data, yielding a time constant $\lambda = 23$ min. Scale bars are 5 μm in each image.

Five minutes after injecting MBP solution at concentrations between 0.5 μg/mL and 500 μg/mL into the fluid cell onto an acidic lipid bilayer (type I), elevations were observed that became more numerous and larger with increasing MBP concentration (Figure 2). These elevations could not be removed by rinsing with buffer 1. They had a defined height of 1.9 $\pm$ 0.2 nm, often with smaller protrusions in the center (Figure 3 top, Figure 4a, Figure 5a). These protrusions disappeared after a few scans. We interpret the elevations as MBP aggregates of monomolecular thickness attached to the lipid bilayer. The protrusions probably consisted of loosely bound material, which was later on distributed by the AFM tip in subsequent scans. At MBP concentrations higher than 20 μg/mL, image contrast was only obtained in rare cases. In the bottom image of Figure 2, contrast disappears during the scan. The reason for not being able to image MBP at high concentration is probably the strong adherence of MBP to the tip.

Images recorded at different times after adding MBP to the solution (5 μg/mL) showed that aggregates grow in lateral dimensions, eventually unite (Figure 3), and fill the entire area. The fact that full coverage of type I lipid bilayers could be achieved indicates that a complete lipid demixing (MBP exclusively binding to the negative DOPS lipids) does not occur.

To compare MBP adsorption with lipid bilayers containing differently charged headgroups, we have investigated adsorption to bilayers consisting of lipid mixtures according to Table 1. Figure 4 a–c shows a comparison of features recorded 15 min

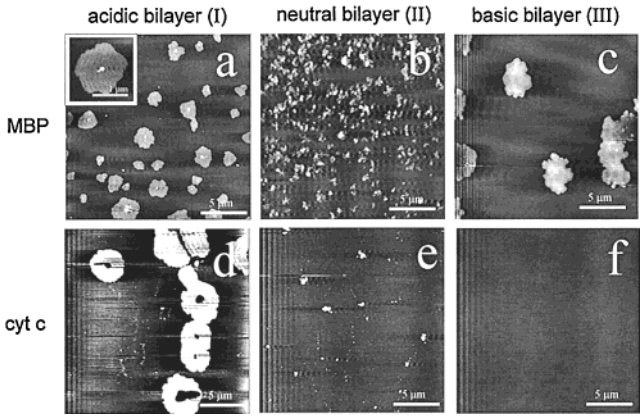

Figure 4. Height images of different lipid bilayer surfaces 15 min after injection of solutions of MBP and cytochrome *c*. Adsorption was investigated on acidic (type I, first column: a, d), purely zwitterionic (type II, second column: b, e), and basic (type III, third column: c, f) lipid bilayers. Protein concentrations were MBP (5 μg/mL (a−c), and cytochrome *c* (d: 0.5 μg/mL; e: 0.5 μg/mL; f: 50 μg/mL). Scan rate was 5 Hz. *Z* scales are 0−10 nm (a−c) and 0−5 nm (d−f).

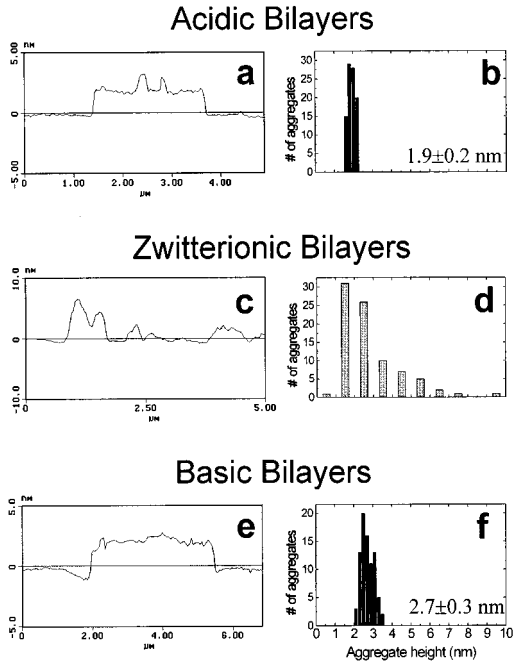

Figure 5. Analysis of MBP aggregate height on acidic, zwitterionic, and basic lipid bilayers. Cross-sections through typical MBP aggregates are given in the left column, distribution of aggregate height is shown in the right column. On acidic and basic lipid bilayers, aggregates exhibited constant height, whereas aggregate height distribution on zwitterionic bilayers is broadly distributed.

after injection of 100 μL of MBP solution (5 μg/mL) on each lipid bilayer surface. MBP aggregate morphology was strikingly different on different lipid bilayer surfaces. On acidic lipid bilayers (type I), flat and almost circular aggregates of radii between 0.2 and 1.5 μm with a height of 1.9 ± 0.2 nm were observed (Figure 4a, Figure 5a,b). The aggregates showed sharp edges and were of constant height over several micrometers (Figure 5a). On many aggregates, additional elevations varying in height (2.5−5 nm) were present near the center (inset, Figure 4a). In some cases, larger aggregates exhibited a considerable amount of irregularly adsorbed material in their center, giving these aggregates a "fried egg"-like appearance (Figure 7a).

On purely zwitterionic lipid bilayers consisting of EPC and cholesterol (type II), aggregates were irregular in height (1.7−10 nm) and two-dimensional morphology (Figure 4b, Figure 5c,d). On basic bilayers (type III), aggregates were large (>2 μm in radius), usually elongated, and 2.7 ± 0.3 nm high (Figure 4c, Figure 5f). MBP aggregate height and morphology observed on the bilayers containing charged headgroups (type I and III) suggest that under the given conditions MBP forms monolayers on these surfaces. This was not the case on zwitterionic bilayers (type II).

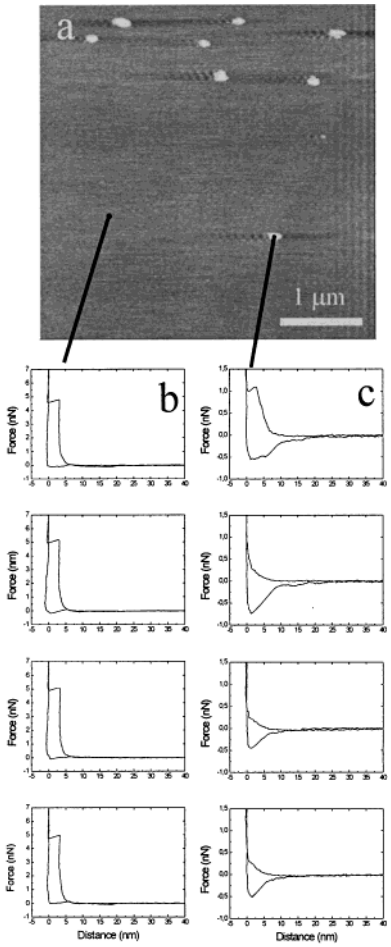

Figure 6. Spatially resolved force spectroscopy on an acidic (type I) bilayer with adsorbed MBP aggregates. (a) Height image of a type I lipid bilayer 15 min after injection of 2 μg/mL MBP solution. (b) Column of four consecutive force curves taken at the indicated position in the flat area of the image. Force curves exhibited behavior as on a bare bilayer (Figure 1d). (c) Column of four consecutive force curves taken on the indicated MBP aggregate. The penetration force was smaller than in (b), the jump vanished during the force scans, and an adhesion of approximately 0.5 nN was observed.

Force Curves. Force curves of MBP-covered lipid bilayers have been reported earlier.[36] A major caveat in that work was that images of MBP adsorbed to the bilayer could not be obtained. Here we report on spatially resolved force spectroscopy by carrying out force scans on bare lipid bilayer and on MBP aggregates during the same experiment. Recording consecutive force curves on bare bilayers, the characteristic jump was observed at a force of approximately 5 nN and force curves did not change over time (Figure 6b). They were indistinguishable from force curves taken on bare bilayers in the absence of MBP.

Force curves taken on MBP aggregates changed with time (Figure 6c). In the first force curve, a jump was always present, although at considerably lower force than on the bare bilayer. This jump disappeared during the following force scans and

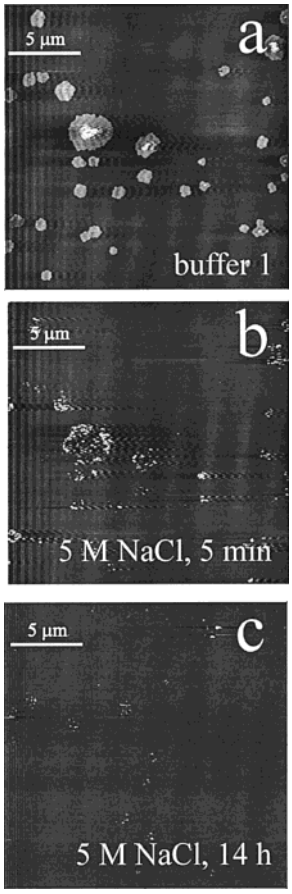

Figure 7. Treatment of MBP aggregates formed on a type I lipid bilayer with 5 M NaCl: the elevations present after 15 min adsorption (a) disappeared after replacement of buffer 1 with 5 M NaCl (b). After 14 h, almost no material was left on the bilayer (c). In contrast, thorough rinsing with buffer 1 did not lead to any changes of the aggregates (not shown).

then reappeared randomly (not shown). An adhesion higher than that observed on the pure bilayer was always present.

The same force curve behavior was observed for MBP on acidic (type I) and basic (type III) lipid bilayers. The behavior is also consistent with earlier results[36] where force curves with and without the jump were observed at the same position, given that in those experiments the lipid bilayer was completely covered with MBP. Force curves observed on MBP aggregates on purely zwitterionic (type II) surfaces were irreproducible, probably because of the irregular adsorption of MBP.

The fact that the characteristic jump disappears upon recording several force curves on an MBP aggregate indicates that the original structure of the phospholipid/MBP layer is locally destroyed by the tip in a force scan. Subsequent force scans would then probe the defect created by the first scan and no bilayer jump could be seen. Over time (in the order of several seconds), the defect healed out so that the jump appeared again in the force curves. This means that the mobility of the MBP/bilayer assembly is reduced as compared with the bare lipid bilayer. This could be termed a "freezing" of the lipid molecules associated with the MBP aggregates. At the same time, the penetration force required to punch through the bilayer during the first approach is reduced by at least 50% as compared with the bare bilayer, resulting from a reduced mechanical stability of the MBP/bilayer assembly toward vertical deformation.

Simple Model for MBP Adsorption to Lipid Bilayers. It has been observed that MBP could be released from myelin by incubation in salt solution.[13] To investigate the effect of a high salt concentration on the aggregates after adsorption in buffer 1, the fluid cell was rinsed with 400 μL of 5 M NaCl solution. This resulted in extensive removal of the aggregates on all bilayer types while the bilayer itself remained intact (Figure 7 on a type I bilayer). Such an observation is usually interpreted as an indication of electrostatic binding. We would, however, like to point out that this should not be understood as a simple reduction of the electrostatic force between MBP and the bilayer, as described by Poisson−Boltzmann continuum theory.[53] The high concentration of ions rather seems to change the structure of ions and water at the interfaces[54] or maybe even the structure of MBP itself. This changed structure leads to an MBP desorption.

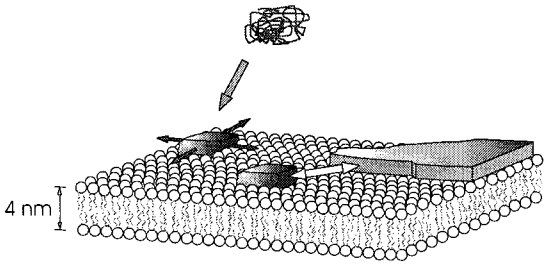

Figure 8. Suggested model for MBP adsorption on acidic lipid bilayers. Solvated MBP molecules adsorb to the lipid bilayer and refold. The adsorbed molecule can diffuse on the bilayer. An attractive interaction between the adsorbed molecules leads to formation of MBP monolayers on the lipid bilayer. Smaller aggregates drift until they hit an obstacle and get stuck. Thus, large, immovable monolayer aggregates form.

The formation of largely continuous monolayers might be explained by a simple model (Figure 8). We assume an attractive interaction between the solvated MBP molecules and the lipid bilayer such that adsorption is favorable. Once adsorbed, the individual MBP molecules are able to diffuse randomly on the bilayer because at room temperature the bilayers were in the fluid phase. Furthermore, we postulate a lateral attraction between the adsorbed MBP molecules. Then randomly diffusing molecules form aggregates. The initial presence of small protrusions in the center of the aggregates suggests that the molecules diffuse until they hit an obstacle and get stuck. This idea is supported by the finding that we could sometimes artificially grow aggregates in designated positions by penetrating the lipid bilayer with the tip several times. Nuclei for spontaneous adsorption were either present before MBP adsorption or might be MBP in a different state from the rest of the patch. The different shapes of the aggregates on different lipid layers could thus be due to (a) different interaction between MBP and the various lipid compositions or (b) a different attractive interaction between the diffusing molecules. The fact that MBP forms monolayers with a defined height on acidic and basic bilayers indicates that on these bilayers the interaction between adsorbed MBP molecules is stronger than between an adsorbed and a free MBP molecule in solution. In addition, the MBP molecules have to assume a certain defined structure on the lipid bilayer. In contrast, on neutral bilayers MBP adsorbed in a comparatively random and unspecific fashion.

These observations agree with the finding that solvated MBP has a different conformation than MBP being in contact with lipid molecules.[21,23] This fact might explain the notion that MBP−MBP interaction of MBP molecules attached to the lipid bilayer should be stronger than that between solvated MBP molecules. Otherwise, MBP could aggregate in solution and adsorb to the bilayer as a three-dimensional aggregate.

The fact that the positively charged MBP molecules adsorb to the like-charged basic (type III) bilayers means that in this

adsorption process, a nonelectrostatic interaction is dominant. This is probably not a simple van der Waals attraction because the structure of MBP adsorbed to mica is different from the structure of MBP adsorbed to basic lipid bilayers. On mica, force-versus-distance measurements showed that MBP behaves like a randomly coiled polymer.[36] MBP on lipid bilayers showed a completely different behavior. Thus the lipid bilayer must exhibit some property that allows MBP to adsorb and refold. This property could be involved with some specific interaction between MBP and lipid headgroups or, alternatively, hydrophobic interaction with the bilayer core. Because to our knowledge no specificity for MBP interaction with lipid headgroups has been reported, we believe that it is the presence of the hydrophobic core that causes the MBP refolding. To "feel" the bilayer core, the molecule must penetrate the headgroup region of the bilayer.

The ability of MBP to interact nonelectrostatically with zwitterionic and basic lipid bilayers does not necessarily mean that such an interaction is also dominant in the adsorption process to acidic (type I) lipid bilayers. If, as suggested above, the presence of the hydrophobic core is indeed causing MBP to refold upon adsorption, we think it is very likely that MBP adsorption to acidic (type I) lipid bilayers also involves a nonelectrostatic component.

Weak interaction between phosphatidylcholine and MBP has been reported by Roux et al.[55] Our observations confirm that such an interaction is present, because MBP does adsorb to an EPC/cholesterol bilayer. Unlike Roux et al., we did not observe a fragmentation of bilayers upon MBP binding. A possible reason could be that in our case the bilayers were supported by the solid substrate, whereas Roux et al. did experiments on lamellar dispersions. Furthermore, the presence of 30% cholesterol in our bilayers adds to bilayer stability and may thus prevent rupture.

Adsorption of BSA and Cytochrome *c* to Lipid Bilayers. For comparison, experiments with BSA, and cytochrome *c* instead of MBP were carried out. For bulk concentrations of BSA up to 500 μg/mL, no aggregate formation was observed on either type of bilayer (not shown).

Cytochrome *c* formed extensive, ring-shaped aggregates with a defined thickness on type I bilayers even at concentrations as low as 0.5 μg/mL (Figure 4d). Hence, it adsorbs more strongly than MBP. Aggregate height was 3.3 ± 0.2 nm. Because the aggregate height is consistent with the known structure of the protein (about 3.4 nm for the longest dimension[30]), we found no indication that cytochrome *c* penetrates significantly into the lipid bilayer. This is in contrast to conclusions of other authors. To explain results of differential scanning calorimetry, surface plasmon resonance spectroscopy, and cyclic voltammetry, it has been suggested that after electrostatic adsorption to the membrane, the cytochrome *c* molecule is able to penetrate partly or completely into the hydrophobic core of the bilayer.[33] A possible explanation for the discrepancy is the different experimental conditions. We used a lower protein concentration and our bilayers contained a significant amount of cholesterol.

The aggregates were difficult to image and were easily deformed or destroyed by scanning, even at low imaging forces of 0.2 nN. Because of this, reliable spatially resolved force curves could not be obtained. On type II lipid bilayers, that is, in the absence of negatively charged lipid headgroups, only small aggregates of the same constant height were observed (Figure 4e). On basic type III lipid bilayers no cytochrome *c* aggregates could be found, even in the presence of cytochrome *c* concentrations of up to 50 μg/mL (Figure 4f). In contrast to MBP behavior, the amount of adsorbed cytochrome *c* decreased continuously over the three systems comprised of acidic, zwitterionic, and basic bilayers. The cytochrome *c* aggregates disappeared upon rinsing with 5 M NaCl. These results are consistent with the observations of Kimelberg et al.,[31] who suggested an electrostatic mechanism for cytochrome *c* adsorption to the membrane.

Domain formation of cytochrome *c* adsorbing to acidic lipid bilayers has already been observed by Haverstick and Glaser[56] at low salt concentrations using fluorescence/optical microscopy on vesicle suspensions. These authors reported aggregation of the negatively charged lipids in those regions where cytochrome *c* had adsorbed. When the low-salt buffer was replaced with 100 mM NaCl buffer, the lipid demixing remained but adsorbed cytochrome *c* could not be detected any more. The authors also reported that cytochrome *c* binding and lipid demixing did not occur when they used 100 mM NaCl solution as the starting buffer. In this work, we have directly shown that cytochrome *c* does adsorb to an acidic lipid bilayer also at an ionic strength of 150 mM NaCl. It is probable that Haverstick and Glaser were not able to detect cytochrome *c* monolayers because of insufficient light attenuation by absorption of the cytochrome *c* heme group.

Conclusion

We have demonstrated that adsorption of MBP and cytochrome *c* to supported lipid bilayers in the liquid/liquid crystalline state can be investigated by AFM in physiological buffer. The morphology of MBP aggregates on lipid bilayers depends on the specific bilayer composition. On negatively charged bilayers used as simple models for the native myelin membrane, MBP formed monolayers of 1.9 ± 0.2 nm height. If a sufficient concentration of MBP was present (10−20 μg/mL), the MBP monolayer covered the entire lipid bilayer. MBP aggregates could be removed from the lipid bilayers in 5 M NaCl. The binding of MBP to lipid bilayers is not only dominated by electrostatic forces, but other interactions must also be significant.

Cytochrome *c* adsorbed to acidic lipid bilayers at low concentrations (approximately 0.5 μg/mL) under physiological ionic strength and formed extensive monolayers of 3.3 ± 0.2 nm height that were sensitive to mechanical distortion by the scanning tip. The higher rigidity of MBP aggregates toward the scanning tip is consistent with the different physiological roles of the proteins. Cytochrome *c* must be able to diffuse on the membrane to be able to act as a carrier of electrons between cytochrome bc_1 and cytochrome *c* oxidase in the mitochondrial respiratory chain. In contrast, MBP is thought to stabilize the apposing cytoplasmic membranes in myelin. The adsorption of cytochrome *c* to lipid bilayers can be explained by a dominating electrostatic interaction.

Acknowledgment. We gratefully acknowledge the careful review and valuable comments (especially on the interpretation of protrusions and MBP adsorbing to a basic membrane) of two anonymous referees. H.M. acknowledges support by the Deutsche Forschungsgemeinschaft.

References and Notes

(1) (a) Garland, P. B. *Q. Rev. Biophys.* **1996**, *29*, 91−117. (b) Knoll, W. *Ann. Rev. Phys. Chem.* **1998**, *49*, 569−638.

(2) Stamm, M. *Scattering in Polymeric and Colloidal Systems*. Mortenson, K., Brown, W., Eds. Gordon & Breach: Longhorne, PA, 1998; Chapter 12.

(3) Johannsmann, D. *Macromol. Chem. Phys.* **1999**, *200*, 501−516.

(4) Huxley, A. F.; Stampell, R. Evidence for saltatory conduction in peripheral myelinated nerve fibers. *J. Physiol. (London)* **1949**, *108*, 315.

(5) Readhead C.; Popko, B.; Takahashi, N.; Shine, S. H.; Saavedra, R. A.; Sidman, P. L.; Hood, L. Expression of a myelin basic protein gene in transgenic mice: correction of the dysmyelination phenotype. *Cell* **1987**, *48*, 703−712.

(6) Campagnoni, A. T. Molecular biology of myelin proteins from the central nervous system. *J. Neurochem.* **1988**, *51*, 1−14.

(7) (a) Staugaitis, S. M.; Colman, D. R.; Pedraza, L. *Bioessays* **1996**, *18*, 13−18. (b) Pedraza, L. L.; Fidler, L.; Staugaitis, S. M.; Colman, D. R. *Neuron* **1997**, *18*, 579−589.

(8) (a) Epand, R. M. *Neuronal and Glial Proteins: Structure, Function and Clinical Application*; (Marangos, P. J., Campbell, I. C., Cohen, R. M., Eds. Academic Press: San Diego, 1988; pp 231−265. (b) Fraser, P. E.; Rand, R. P.; Deber, C. M. *Biochim. Biophys. Acta* **1989**, *983*, 24−29.

(9) Smith, R. *Biochim. Biophys. Acta* **1977**, *491*, 581−590.

(10) Boggs, J. M., Wood, D. D.; Moscarello, M. A. *Biochemistry* **1981**, *20*, 1065−1073.

(11) Sankaram, M. B.; Brophy, P. J.; Marsh, D. *Biochemistry* **1991**, *30*, 5866−5873.

(12) (a) Smith, R.; Braun, P. E.; Low, M. G.; Ferguson, M. A. J.; Sherman, W. R. *Biochem. J.* **1987**, *248*, 285−288. (b) McLaurin, J.; Hew, C.; Moscarello, M. A. *Biochem. J.* **1990**, *269*, 278−279.

(13) (a) Eng, L. F.; Chao, F.-C.; Gersh, B.; Pratt, D.; Tavaststjerna, M. G. *Biochemistry* **1968**, *7*, 4455−4465. (b) Glynn, P.; Chantry, A.; Groome, N.; Cuzner, M. L. *J. Neurochem.* **1987**, *48*, 752−759. (c) Smith, R.; Braun, P. E. *J. Neurochem.* **1988**, *50*, 722−729.

(14) (a) Lampe, P. D.; Wei, G. J.; Nelsestuen, G. L. *Biochemistry* **1983**, *22*, 1594−1599. (b) Sedzik, J.; Blaurock, A. E.; Höchli, M. *J. Mol. Biol.* **1984**, *174*, 385−409. (c) Surewicz, W. K.; Epand, R. M.; Epand, R. F.; Hallet, F. R.; Moscarello, M. A. *Biochim. Biophys. Acta* **1986**, *863*, 45−52. (d) Páli, T.; Ebert, B.; Horvath, L. I. *Biochim. Biophys. Acta* **1987**, *904*, 364−352. (e) Maggio, B.; Yu, R. K. *Chem. Phys. Lipids* **1989**, *51*, 127−136. (f) Maggio, B.; Yu, R. K. *Biochim. Biophys. Acta* **1992**, *1112*, 105−114. (g) Jo, E.; Boggs, J. M. *Biochemistry* **1995**, *34*, 13705−13716.

(15) Lampe, P. D.; Nelsestuen, G. L. *Biochim. Biophys. Acta* **1982**, *693*, 320−325.

(16) MacNaughtan, W.; Snook, K. A.; Caspi, E.; Franks, N. P. *Biochim. Biophys. Acta* **1985**, *818*, 132−148.

(17) (a) Cheifetz, S.; Moscarello, M. A. *Biochemistry* **1985**, *24*, 1909−1914. (b) Surewicz, W. K.; Moscarello, M. A.; Mantsch, H. H. *Biochemistry* **1987**, *26*, 3881−3886. (c) Nezil, F. A.; Bayerl, S.; Bloom, M. *Biophys. J.* **1992**, *61* 1413−1426. (d) Smith, R. *J. Neurochem.* **1992**, *59*, 1589−1608. (e) Boggs, J. M.; Rangaraj, G.; Koshy, K. M. *Biochim. Biophys. Acta* **1999**, *1417*, 254−266.

(18) Reinl, H. M.; Bayerl, T. M. *Biochim. Biophys. Acta* **1993**, *1151*, 127−136.

(19) Sedzik, J.; Kirschner, D. A. *Neurochem. Res.* **1992**, *17*, 157−166.

(20) Blodgett, K. B. *J. Am. Chem. Soc.* **1935**, *57*, 1007−1022.

(21) Haas, H.; Torrielli, M.; Steitz, R.; Cavatorta, P.; Sorbi, R.; Fasano, A.; Riccio, P.; Gliozzi, A. *Thin Solid Films* **1998**, *327*−*329*, 627−631.

(22) (a) Krigbaum, W. R.; Hsu, T. S. *Biochemistry* **1975**, *14*, 2542−2546. (b) Gow, A.; Smith, R. *Biochem. J.* **1989**, *257*, 535−540.

(23) (a) Keniry, M. A.; Smith, R. *Biochim. Biophys. Acta* **1979**, *578*, 381−391. (b) Keniry, M. A.; Smith, R. *Biochim. Biophys. Acta* **1981**, *668*, 107−108. (c) Mendz, G. L.; Moore, W. J.; Brown, L. R.; Martenson, R. E. *Biochemistry* **1984**, *23*, 6041−6046. (d) Mendz, G. L.; Brown, L. R.; Martenson, R. E. *Biochemistry* **1990**, *29*, 2304−2311. (e) Mendz, G. L.; Miller, D. J.; Ralston, G. B. *Eur. Biophys. J.* **1995**, *24*, 39−53.

(24) (a) Papahadjopoulos, D.; Moscarello, M.; Eylar, E. H.; Isac, T. *Biochim. Biophys. Acta* **1975**, *401*, 317−335. (b) Boggs, J. M.; Moscarello, M. A. *J. Membr. Biol.* **1978**, *39*, 75−96. (c) Boggs, J. M.; Rangaraj, G.; Moscarello, M. A.; Khoshy, K. M. *Biochim. Biophys. Acta* **1985**, *816*, 208−220. (d) Boggs, J. M.; Chia, L. S.; Rangaraj, G.; Moscarello, M. A. *Chem. Phys. Lipids* **1986**, *39*, 165−184.

(25) Boggs, J. M.; Moscarello, M. A.; Papahadjopoulos, D. *Biochemistry* **1977**, *16*, 5420−5426.

(26) Sankaram, M. B.; Brophy, P. J.; Marsh, D. *Biochemistry* **1989**, *28*, 9699−9707.

(27) Beniac, D. R.; Luckevich, M. D.; Czarnota, G. J.; Tompkins, T. A.; Ridsdale, R. A.; Ottensmeyer, F. P.; Moscarello, M. A.; Harauz, G. *J. Biol. Chem.* **1997**, *272*, 4621−4268.

(28) ter Beest, M. B. A.; Hoekstra, D. *Eur. J. Biochem.* **1993**, *211*, 689−696.

(29) Tanford, C. *The Hydrophobic Effect*. Wiley: New York, 1973, p 97.

(30) (a) Takano, T.; Kallai, O. B.; Swanson, R.; Dickerson, R. E. *J. Biol. Chem.* **1973**, *248*, 5234−5255. (b) Bushnell, G. W.; Louie, G. V.; Brayer, G. D. *J. Mol. Biol.* **1990**, *214*, 585−595.

(31) Kimelberg, H. K.; Leed, C. P.; Claude, A.; Mrena, E. *J. Membr. Biol.* **1970**, *2*, 235−251.

(32) (a) Brown, L. R.; Wüthrich, K. *Biochim. Biophys. Acta* **1977**, *468*, 389−410. (b) Szebeni, J.; Tollin, G. *Biochim. Biophys. Acta* **1988**, *932*, 153−159. (c) Spooner, P. J. R.; Watts, A. *Biochemistry* **1991**, *30*, 3871−3879. (d) Zhang, F.; Rowe, E. S. *Biochim. Biophys. Acta* **1994**, *1193*, 219−225.

(33) (a) Salamon, Z.; Tollin, G. *Biophys. J.* **1996**, *71*, 848−857. (b) Salamon, Z.; Tollin, G. *J. Bioenerg. Biomembr.* **1997**, *29*, 211−221.

(34) Van, S. P.; Griffith, O. H. *J. Membr. Biol.* **1975**, *20*, 155−170.

(35) Voet, D.; Voet, J. G. *Biochemistry*; VCH: Cambridge, U.K., 1992.

(36) Mueller, H.; Butt, H.-J.; Bamberg, E. *Biophys. J.* **1999**, *76*, 1072−1079.

(37) Siedle, P.; Butt, H.-J.; Bamberg, E.; Wang, D. N.; Kühlbrand, W.; Zach, J.; Haider, M. *Inst. Phys. Conf. Ser.* **1993**, *130*, 361−364.

(38) (a) Cleveland, J. P.; Manne, S.; Bocek, D.; Hansma, P. K. *Rev. Sci. Instrum.* **1993**, *64*, 403−405. (b) Preuss, M.; Butt, H.-J. *Langmuir* **1998**, *14*, 3164−3174.

(39) Jaschke, M.; Butt, H.-J. *Rev. Sci. Instrum.* **1995**, *66*, 1258−1259.

(40) Butt, H.-J.; Jaschke, M.; Ducker, W. A. *Bioelectrochem. Bioenerg.* **1995**, *38*, 191−201.

(41) Hoh, J. H.; Engel, A. *Langmuir* **1993**, *9*, 3310−3312.

(42) (a) Brian, A. A.; McConnell, H. M. *Proc. Natl. Acad. Sci. U.S.A.* **1984**, *81*, 6159−6163. (b) McConnell, H. M.; Watts, T. H.; Weis, R. M.; Brian, A. A. *Biochim. Biophys. Acta* **1986**, *864*, 95−106. (c) Mou, J.; Yang, J.; Shao, Z. *Biochemistry* **1994**, *33*, 4439−4443. (d) Ohlsson, P.; Tjärnhage, T.; Herbai, E.; Löfås, S.; Puu, G. *Bioelectrochem. Bioenerg.* **1995**, *38*, 137−148. (e) Keller, C. A.; Kasemo, B. *Biophys. J.* **1998**, *75*, 1397−1402.

(43) Mou, J.; Yang, J.; Huang, C.; Shao, Z. *Biochemistry* **1994**, *33*, 9981−9985.

(44) (a) Parsegian, V. A.; Fuller, N.; Rand, R. P. *Proc. Natl. Acad. Sci. U.S.A.* **1979**, *76*, 2750−2754. (b) McIntosh, T. J.; Simon, S. A. *Biochemistry* **1986**, *25*, 4058−4066.

(45) (a) Pashley, R. M. *J. Colloid Interface Sci.* **1981**, *80*, 153−162. (b) Pashley, R. M. *J. Colloid Interface Sci.* **1981**, *83*, 531−546.

(46) Marra, J.; Israelachvili, J. *Biochemistry* **1985**, *24*, 4608−4618.

(47) McIntosh, T. J.; Magid, A. D.; Simon, S. A. *Biochemistry* **1987**, *26*, 7325−7332.

(48) Leikin, S.; Parsegian, V. A.; Rau, D. C. *Annu. Rev. Phys. Chem.* **1993**, *44*, 369−395.

(49) Israelachvili, J. N.; Wennerström, H. *Nature* **1996**, *379*, 219−225.

(50) Ducker, W. A.; Clarke, D. R. *Colloids Surf., A* **1994**, *94*, 275−292.

(51) Marsh, D. *Handbook of Lipid Bilayers;* CRC Press: Boca Raton, FL, 1990; p 125.

(52) Käsbauer, M.; Junglas, M.; Bayerl, T. M. *Biophys. J.* **1999**, *76*, 2600−2605.

(53) McLaughlin, S. *Annu. Rev. Biophys. Biophys. Chem.* **1989**, *18*, 113−136.

(54) Cevc, G. *Biochim. Biophys. Acta* **1990**, *1031*, 311−382.

(55) Roux, M.; Nezil, F. A.; Monck, M.; Bloom, M. *Biochemistry* **1994**, *33*, 307−311.

(56) Haverstick, D. M.; Glaser, M. *Biophys. J.* **1989**, *55*, 677−682.